In vitro and in vivo study on the anticancer effects of anethole-loaded bovine serum albumin nanoparticles surface decorated with chitosan and folic acid

Farzaneh Sadeghzadeh[1], Hasti Nasiraei Haghighi[2], Mahdiyeh Ghiyamati[2], Fateme Hajizadenadaf[2] and Masoud Homayouni Tabrizi[2*]

*Correspondence:
mhomayouni6@gmail.com;
mhomayouni6@mshdiau.ac.ir

[1] Department of Biochemistry, Neyshabur Branch, Islamic Azad University, Neyshabur, Iran
[2] Department of Biology, Mashhad Branch, Islamic Azad University, Mashhad, Iran

Abstract

Anethole (Ant) is a herbal compound with unique properties, which is limited in its clinical use due to its low solubility in aqueous solutions. Therefore, in this study, albumin nanocarrier modified with chitosan-folate was used to transfer Ant to cancer cells and its anticancer effects were evaluated. First, Ant was loaded on albumin nanoparticles by desolvation method and then the surface of nanoparticles was covered with chitosan bound to folate. After characterization, the amount of Ant loading in nanoparticles was measured by the absorption method and then its toxicity effects on breast cancer cell lines, colon, and normal cells were evaluated by the MTT method. The real-time QPCR method was used to investigate the expression changes of apoptosis-related genes in the treated cells compared to the control cells, and finally, the antitumor effects of nanoparticles were evaluated in the mouse model carrying breast cancer. The results of this investigation showed the presence of nanoparticles with dimensions of 252 nm, a dispersion index of 0.28 mV, and a surface charge of 27.14 mV, which are trapped in about 88% of ATL. The toxicity effect of nanoparticles was shown on breast, colon, and normal cancer cells, respectively. In addition, the examination of the gene profile under investigation showed an increase in the expression of BAX and caspase-3 and -9 along with a decrease in the expression of the Bcl-2 gene, which confirms the activation of the internal pathway of apoptosis. The decrease in the volume of tumors and the presence of apoptotic areas in the tissue sections confirmed the antitumor effects of nanoparticles in the in vivo model. The inhibition percentage of free Ant and nanoparticles with a concentration of 25 and 50 mg/kg/tumor volume was reported as 36.9%, 56.6%, and 64.9%, respectively, during 15 days of treatment. These results showed the effectiveness of the formulation in inhibiting cancer cells both in vitro and in vivo.

Keywords: Anethole, Active targeting, Cancer, BSA nanoparticles, Chitosan coating

Introduction

Conventional cancer treatment involves surgery, in conjunction with chemo- and radio-therapy if necessary (Satapathy et al. 2023). Despite their efficiency, both medications have significant adverse effects, which limit their use (Maleki et al. 2019). It is, therefore, possible for these treatments to be more aggressive and to cause numerous unwanted side effects as well as negative effects on the cells in the body other than cancerous cells (Mirhadi et al. 2020). It is possible to reduce these adverse effects using plant products as complementary treatments, in conjunction with a reduction in exposure to chemo-therapy and radiotherapy (Greenwell and Rahman 2015).

Traditionally, flavored plants have been used as homeopathic remedies to treat a variety of diseases, including cancer. It has been found that herbal ingredients possess the ability to inhibit the proliferation of cancer cells as well as to reduce the side effects associated with chemotherapy and radiotherapy. Hence, traditional medicine may offer a more effective and specific treatment for cancer than chemotherapy compounds (Zimmermann-Klemd et al. 2022).

Anethole (1-methoxy-4-propenyl-benzene, iso-estragole) (Ant) is an alkoxypropylbenzene derivative and an important flavoring component of essential oils from aromatic plants including anise, star-anise, and fennel (Aprotosoaie et al. 2016; Ponte et al. 2012; Huxley 1992). In nature, trans-Ant constitutes around 90% of the naturally occurring isomer form of anethole (Jurado et al. 2006). Around the world, traditional uses of plants that contain Ant are mainly for treating digestive and neurological disorders, and inflammatory conditions of the skin or respiratory tract. Trans-Ant is considered food grade and can mask unpleasant odors, mainly acidic, sour, and sulfurous. Therefore, it is widely used as a masking agent in cosmetics, soaps, and oral hygiene products (toothpaste and mouthwash) is used (Dongare et al. 2012). In addition, Ant is used in food preservation, industrial products, feed additives, artificial flavors, and pesticides (Lal et al. 2022). As a potential antitumor agent, Ant interferes with the biology of cancer cells with its pro-apoptotic, anti-metastatic, and anti-inflammatory effects. Ant and its synthetic analogs show therapeutic activity by suppressing invasive and non-invasive adenocarcinomas (Rhee et al. 2014).

Nanotechnology has proven extremely successful in the delivery of drugs. A consensus definition of nanoparticles has not yet been reached internationally. Particles with sizes ranging from 1 to 100 nm are considered nanomaterials by many sources (Auffan et al. 2009). A growing field of research involves the use of nanotechnology with natural products. It is possible to deliver natural compounds in the treatment of cancer and other chronic human diseases using nanotechnology. Natural products can be made more bioavailable, targeted, and controlled-release by incorporating nanoparticles (Watkins et al. 2015). As a highly water-soluble protein, bovine serum albumin (BSA) binds drugs and inorganic substances noncovalently. By precipitating albumin in organic solvents, and then crosslinking it with glutaraldehyde molecules, microscopic particles and nanoparticles of albumin can be obtained (Tian et al. 2004). The first commercially available albumin nanoparticles with paclitaxel were 130 nm in size (Kratz 2008). According to some studies, hydrophobic compounds are effectively transported by particles with a diameter of 20–200 nm (Xu et al. 2011). It is possible that negative or positive charge molecules could be electrostatically adsorbing to BSA

nanoparticles, and the presence of hydrophobic cavities could facilitate the incorporation of drugs that are insoluble in water (Mohanta et al. 2012; Subia and Kundu 2012). In comparison with liposomal nanocarriers, BSA nanoparticles are smaller and have better-controlled properties for drug delivery (Wei et al. 2014).

Chitosan (CS) has been widely used as a particle-forming polymer and, more innovatively, as a surface coating in pharmaceutical nanotechnology. Several types of nanocarriers have been decorated with CS for a wide variety of applications, including polymeric nanoparticles, lipid nanoparticles, and metal-based nanoparticles (Cé et al. 2016; Gonçalves et al. 2012; Hamedinasab et al. 2020; Fonte et al. 2011; Agotegaray et al. 2016; Frank et al. 2020). Researchers have demonstrated in vitro and in vivo that CS can be used to modify the surface of nanocarriers of these types, improving their physicochemical stability, controlling drug release, and promoting mucoadhesive properties and tissue penetration. Modulating cell interactions, enhancing antimicrobial effects, and enhancing bioavailability and drug efficacy are some of how this can be accomplished.

Through the enhanced permeability and retention (EPR) effect, passive targeting nanoparticles allow drugs to leak from blood vessels supplying cancerous cells (Cho et al. 2008). In contrast, active targeting nanoparticles target ligands conjugated on their surface, thereby increasing the rate of receptor-mediated endocytosis, thus increasing drug accumulation in the tumor microenvironment and cells (Mashreghi et al. 2018, 2021a). Various tumors overexpress folate, making it a cancer-targeting ligand. As cancer progresses, folate receptor density increases. Nanocarriers can be tagged with folic acid (FA) for imaging and diagnosis. Chemotherapeutics can be delivered with FA-decorated nanoparticles (Ebrahimnejad et al. 2022).

This study aimed to prepare and characterize Ant-loaded BSA nanoparticles decorated with FA-bonded CS. After characterization, the in vitro cytotoxicity and real-time qPCR were performed. Then, the anti-tumor effects of Ant-BSA–CS–FA were evaluated on mice-bearing tumor models.

Materials and methods

Materials

Ant, BSA, and MTT were obtained from Sigma Aldrich (Darmstadt Germany). Human foreskin fibroblast (HFF) normal cells and MCF-7 human breast cancer, HT-29 human colon carcinoma, and TUBO mice breast cancer cells were obtained from Ferdowsi University of Mashhad cell bank, Iran. All materials and reagents needed for cell culture were provided by Gibco (USA).

Preparation of the Ant-loaded BSA nanoparticles (Ant-BSA)

For the synthesis of nanoparticles, BSA was first dissolved in 10 mM NaCl and placed on a continuous stirrer for 30 min. Then, the pH of the solution was increased to 8.2. Next, Ant was dissolved in 96% ethanol and added dropwise to BSA. The resulting mixture was placed on the stirrer for 10 min. Next, glutaraldehyde was added to the mixture and it was kept under constant stirring for 24 h.

Surface modification of the Ant-BSA

To modify the surface, chitosan was placed in 1% acetic acid on the stirrer for half an hour, while FA was also activated with 1-ethyl-3-(3-dimethylaminopropyl)carbodiimide (EDC) and *N*-hydroxysuccinimide (NHS). Next, NHS–FA was filtered and added drop-wise to chitosan and kept under constant stirring on a stirrer for 24 h. After 24 h, the pH was adjusted to 9.0 and the precipitate was collected by centrifugation. Next, Ant-BSA and the precipitate of CS–FA in water and 1% acetic acid were mixed and incubated for 2 h under continuous stirring. After that, the Ant-BSA–CS–FA was collected and the supernatant was used to check the amount of drug encapsulation.

Characterization of the Ant-BSA–CS–FA

To check the size and dispersion index of nanoparticles, the dynamic light scattering (DLS) method was used. The surface potential of nanoparticles was also measured using a Zeta sizer device. To evaluate these indicators, nanoparticles were first dissolved in deionized distilled water and then diluted 10 times. After ensuring complete dispersion, the resulting colloidal suspension was analyzed using DLS (Nano-ZS, Malvern, UK). Scanning electron microscope (SEM) microscope was used to evaluate the morphology of nanoparticles. For this purpose, a colloidal suspension was prepared and sprayed on an aluminum grid. After drying, the surface of the nanoparticles was coated with gold and subjected to microscopic examination. Functional groups of nanoparticles were investigated by the Fourier transform infrared (FTIR) spectroscopy. For this purpose, 2 mg of nanoparticles were mixed with KBr powder and then compressed and made into tablets. Tablets were analyzed in a spectrometer in the range of 400 to 5000.

Encapsulation efficiency (EE)

To check the amount of percentage of EE (EE%), an indirect method and absorption spectrophotometer was used. First, different concentrations of Ant were prepared and their absorption was measured at a wavelength of 259 nm and its standard curve was plotted. By placing the absorption of the supernatant in the resulting formulation, the amount of free Ant was calculated and the amount of the encapsulated drug was calculated using the following formula:

$$EE\% = (\text{amount of free drug} - \text{the total amount of drug}) \big/ \text{total amount of drug} \times 100.$$

Cytotoxicity of the Ant-BSA–CS–FA

The MTT method was used to investigate the toxicity effect of nanoparticles. This method is a colorimetric method and it is easy to reduce yellow tetrazolium salt by dehydrogenase enzyme of living cells and produce purple formazan crystals. For this purpose, 5000 cells were transferred to each well of a 96 plate and after 24 h of incubation, the cells were treated in three replicates with different concentrations of nanoparticles. After 48 h of treatment, the cell culture medium was drained and 100 μL of MTT solution in the culture medium were added to each well. After 4 h of incubation and depletion of media, 100 μL of Dimethyl sulfoxide (DMSO) were added to each well and analyzed under the ELISA reader device. The following formula was used to check the viability of the cells and IC50 values were calculated using CalcuSyn version 2.0:

Sadeghzadeh *et al. Cancer Nanotechnology*   (2023) 14:24

Page 5 of 15

$$\text{Cell viability}(\%) = \left(\text{absorbance of sample} / \text{absorbance of cells without treatment}\right) \times 100.$$

Anti-apoptotic properties of the Ant-BSA–CS–FA using real-time qPCR

The expression levels of four genes including Caspase-3, Caspase-9, Bcl-2, and BAX were evaluated in this study. The primers list is shown in Table 1. For this purpose, first, the cells were transferred from the culture flask to four new culture flasks and after 48 h they were treated with different concentrations of nanoparticles for 48 h. After the treatment period, the total RNA of the cells was extracted using an RNA extraction kit according to the manufacturer's protocol. Next, the amount of RNA to prepare cDNA was measured by the nanodrop method, and a specific volume of RNA was used for cDNA synthesis. One microliter of cDNA was synthesized in specific concentrations along with 10 μL of SYBR green, 3 μL of water, and 2 μL of primer to prepare the reaction mixture. Using real-time qPCR, the amounts of gene expressions were analyzed.

In vivo anti-tumor activities of the Ant-BSA–CS–FA

For this purpose, 32 BALB/s female mice aged approximately 4–8 weeks and weighing 18–23 g were purchased from the animal department of the Pasteur Institute of Iran, Tehran, Iran. After 1 week of keeping in new conditions and adaption, the anti-tumor test was performed.

TUBO mouse breast cancer cells were used to prepare the cell suspension required for injection. The cells were cultured in 20% Dulbecco's Modified Eagle Medium (DMEM) culture medium until they reached the logarithmic phase, and then they were separated from the flasks and the number of cells was counted. Next, 300,000 cells were injected in a volume of 100 μL at the flanked area of each mouse. The mice were examined for 1 week in terms of tumor formation and after confirming the presence of tumors, the mice were divided into 4 groups of 8 each (the first group included control mice without treatment, the second group receiving free-drug, and the third and fourth groups receiving 25 and 50 mg/dose of Ant-BSA–CS–FA, respectively, by intraperitoneal injection (i.p.) every day for 15 days. On the first day of treatment, the size of the tumors was evaluated and recorded using a digital caliper. Finally, after the treatment period, chloroform was used to anesthetize the animals and then the tumors were removed and transferred to 10% formalin for histological evaluations.

After undergoing histological preparations including, fixation, embedding, and sectioning, the samples were stained in hematoxylin and eosin (H&E) staining, in which the acidic components of the cell such as the nucleus, nucleic acids (DNA and RNA)

Table 1 List of primers used in real-time qPCR

Gene	Forward	Reverse
GAPDH	GCAGGGGGGAGCCAAAAGGGT	TGGGTGCCAGTGATGGCATGG
Bax	AAACTGGT GCTCAAGGCCC	CTTCAGTGACTCGGC CAGG
Bcl-2	GATAACGGAGGCTGGGATGC	TCACTTGTGGCCCAGATAGG
Caspase-3	CTGGACTGTGGCATTGAGAC	ACAAAGCGACTGGATGAACC
Caspase-9	CCAGAGATTCGCAAACCAGAGG	GAGCACCGACATCACCAAATCC

are stained with the basic dye of hematoxylin and the basic parts of the cell (cytoplasm) are stained with the color of this eosin dye with acidic property to evaluate the tissue. In this way, the cytoplasm of stained tissues is pink and the nucleus is dark, blue, or purple. Finally, the slides were covered with a coverslip and subjected to microscopic examination.

Statistical analysis

The data were analyzed using the GraphPad Prism software (version 8) and a one-way ANOVA test. To analyze variance and compare means, the LSD method was used. A significance level of $p < 0.05$ was used to determine the significance of the results.

Results

Characterization

Examining the particle size by the DLS method showed that the formed nanoparticles have a hydrodynamic diameter of 252 nm with a dispersion index of 0.28 (see Fig. 1A). The nanoparticles' small size and narrow dispersion distribution indicate the synthesis of nanoparticles with high stability. The Zeta potential of nanoparticles with a zeta sizer is shown in Fig. 1B. This indicator was reported as 27.14 mV, indicating the formation of high-stability nanoparticles. The positive surface charge of nanoparticles can be attributed to the presence of chitosan coating around the particles. Examining the morphology of nanoparticles with an SEM microscope, as shown in Fig. 1C, showed the presence of multi-faceted and multi-shaped nanoparticles that have a smooth surface. Examining the size of the particles shows that the size of most of the particles is consistent with the data of the DLS report. In this study, BSA nanoparticles modified with CS–FA loaded with Ant were analyzed by the FTIR method to check the presence of functional groups. The results of this investigation shown in Fig. 1D, in which the presence of characteristic
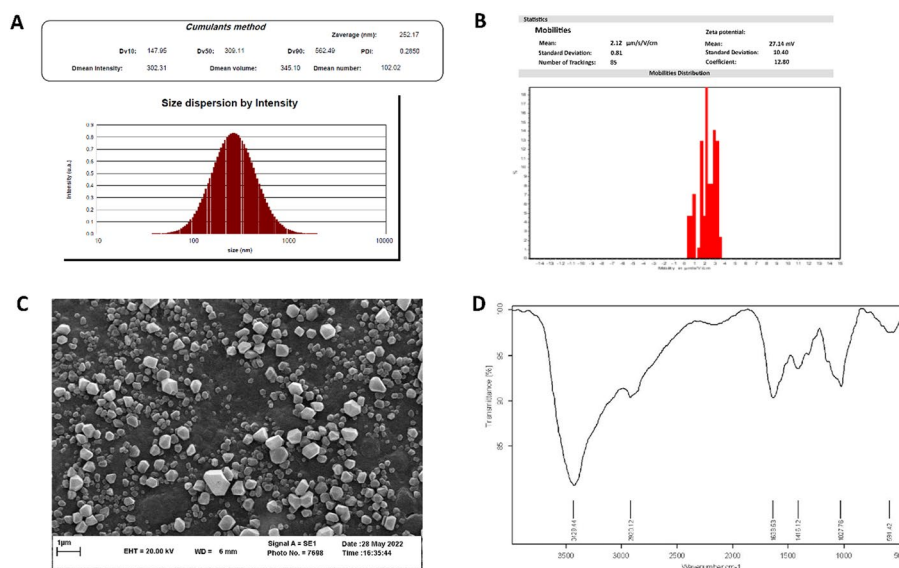

Fig. 1 Characterization. **A** Results of DLS reports indicated the *Z*-average of 252 nm. **B** Result of the zeta-potential of the Ant-BSA–CS–FA, **C** SEM micrograph of the Pip–Ag–BSA–NP, and **D** FTIR spectra of the Ant-BSA–CS–FA

peaks of CS in the region of 3429 cm^{-1} concerning the stretching of hydrogen bonds between OH and NH molecules in chitosan and peaks in the range of 1638 cm^{-1} related to the C=O vibration of acetyl groups in CS (Amide I). The Amide III band at 1416 cm^{-1} is due to a combination of NH deformation and CN stretching vibration, and the 1027 cm^{-1} peak corresponding to C–O stretching vibration was also observed. The presence of CS groups and small changes in their peaks confirm the formation of nanoparticles with CS coating. The EE% of Ant was reported to be 88.7%, which shows the high efficiency of the prepared formulation.

Cytotoxicity studies

The cytotoxic effect of Ant-BSA–CS–FA on normal HFF skin cells is shown in Fig. 2A. As can be seen, up to a concentration of 250 µg/mL, no toxic effects were observed against normal cells, while at concentrations below 200 µg/mL, both cancer cells were inhibited by more than 50% (see Fig. 2B, C). These results show the effectiveness of the treatment against cancer cells. The safety of nanoparticles on normal cells below the concentration of 250 µg/mL was shown by the MTT method. Examining the toxicity effect of nanoparticles in colon cancer cells showed an IC50 of about 175 µg/mL. In other words, 50% of cancer cells were inhibited at a concentration of 175 µg/mL of nanoparticles (see Fig. 2B). The inhibitory effect of nanoparticles on cells was reported in a concentration-dependent manner. The toxicity effect of nanoparticles on breast cancer
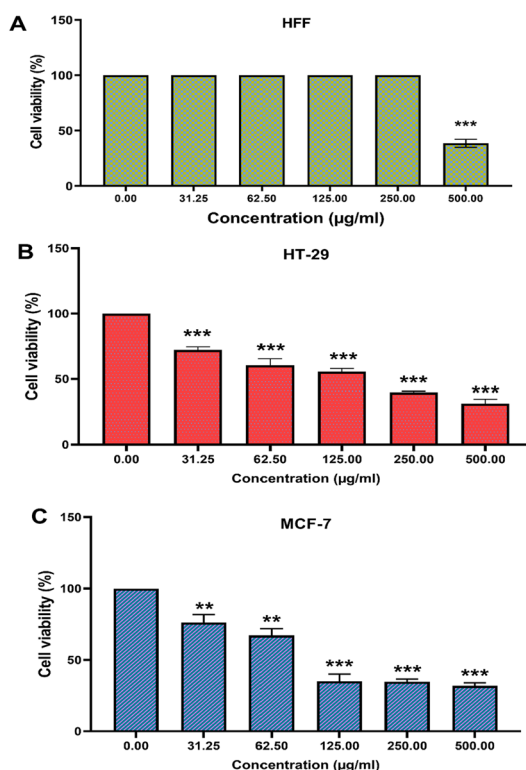

Fig. 2 Cytotoxicity effects of Ant-BSA–CS–FA. **A** Cell viability diagrams of the HFF normal cells, **B** HT-29 colon carcinoma cells, and **C** MCF-7 breast cancer cells treated with various concentrations of Ant-BSA–CS–FA. (**p < 0.01, and ***p < 0.001). The test was performed in triplicate. The data were shown as mean ± SD

cells is shown in Fig. 2C. The results of this study showed a concentration-dependent reduction of nanoparticles against cancer cells. As shown in the graph, the IC50 of 96.6 μg/mL, and at this concentration, 50% of cancer cells have undergone apoptosis. In the highest concentration of 70%, the inhibitory effect of nanoparticles against the investigated cells has been shown. In addition, the comparison of the inhibition rate of nanoparticles against two cell lines showed higher inhibition of nanoparticles on breast cancer cells.

Real-time qPCR

The caspase-3 gene is common in the intrinsic and extrinsic pathways of apoptosis, and the expression level of this gene changes with the activation of each of the intrinsic and extrinsic pathways. As shown in Fig. 3A, the expression level of this gene has shown a significant increase in all three investigated concentrations (*$p < 0.05$ and **$p < 0.01$), which indicates the occurrence of apoptosis in cells treated with nanoparticles. The caspase-9 gene is activated in the activation of the internal pathway of apoptosis, so the
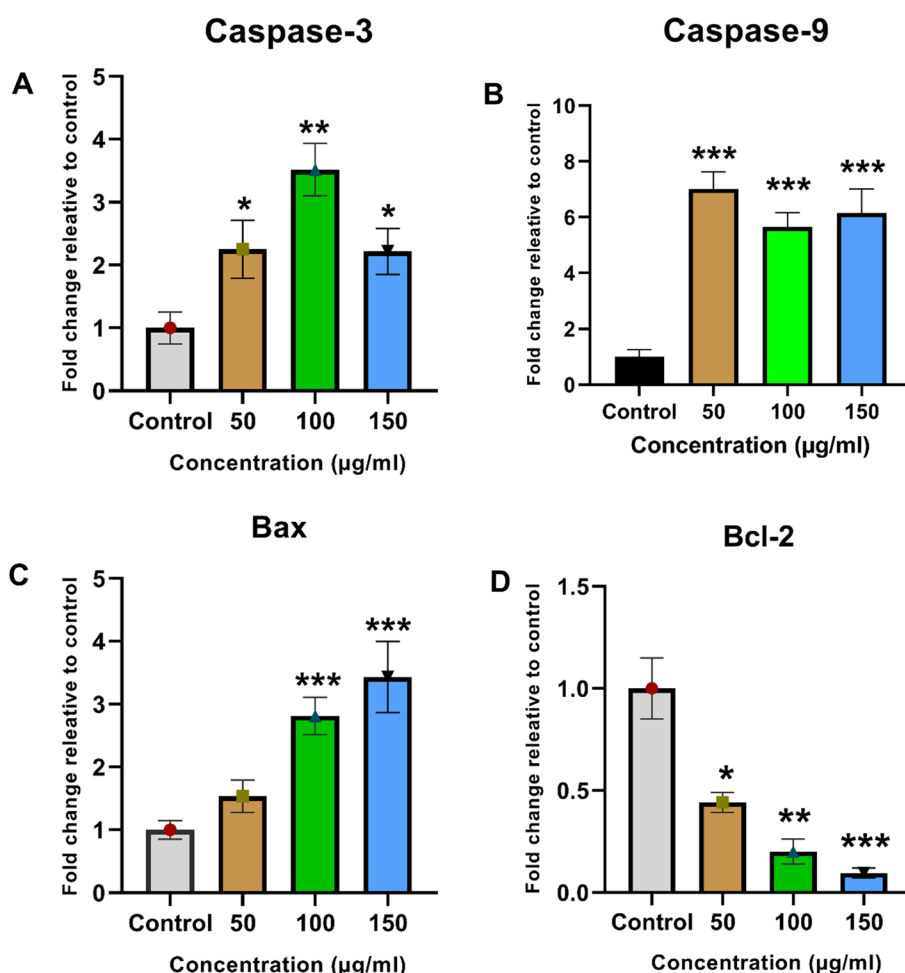

Fig. 3 Real-time qPCR. Quantitative analysis of caspase-3, caspase-9, BAX, and Bcl-2 genes expression in cells treated with Ant-BSA–CS–FA. (*$p < 0.05$, **$p < 0.01$, $p < 0.01$, and ***$p < 0.001$). The data were presented as mean ± SD. The test was performed in triplicate

increase in the expression of this gene in cells treated with nanoparticles indicates the activation of the internal pathway of apoptosis. In other words, increasing the expression of BAX shows the activation of the internal pathway of apoptosis in cells treated with Ant-BSA–CS–FA (see Fig. 3B). Figure 3C shows the changes in the expression of the BAX gene as a pro-apoptotic gene which showed that the expression of this gene in the cells increased in all the treated concentrations; however, only in the concentration of 100 and 150 µg/mL, the increase in expression was shown significantly (***$p < 0.001$). Since the treatment with nanoparticles increased the expression of BAX as a proapoptotic gene, the results show the effect of nanoparticles on the activation of the apoptosis process. The BCL-2 gene is known as an apoptosis inhibitor gene. Therefore, the decrease in the expression of this gene causes the activation of the apoptosis process. The results of this study showed a decrease in the expression of the BCL-2 gene in all three concentrations. As it can be seen that nanoparticles inhibit BCL-2 in treated cells in a concentration-dependent manner, these results show the effectiveness of Ant-BSA–CS–FA in activating the apoptosis process (see Fig. 3D).

In vivo anti-tumor activates

Examining the volume of tumors in samples treated with Ant-BSA–CS–FA compared to control and samples treated with the free drug showed the effectiveness of the formulation in reducing tumor growth. As can be seen in Fig. 4A, the largest decrease in tumor volume is observed in samples treated with a concentration of 50 mg/dose of nanoparticles. Next, nanoparticles with a concentration of 25 mg/dose have shown a high inhibitory effect. The inhibition percentage of free Ant and nanoparticles with a concentration of 25 and 50 mg/kg/tumor volume was reported as 36.9%, 56.6%, and 64.9%, respectively, during 15 days of treatment. Examining the size of the tumors after separating the samples from the body shows a reduction in the size of the tumor in the treated samples compared to the non-treated samples (see Fig. 4B). These results can be related to the effectiveness of Ant-BSA–CS–FA in reducing tumor growth during treatment.

Examining the histological changes in the tumor samples extracted from the treated mice compared to the untreated mice, the effect of nanoparticles is shown in Fig. 5. As can be seen in the picture, the control sample, is uniform and has sections called carcinoma islets, while in the samples treated with the Ant and two doses of Ant-BSA–CS–FA, some carcinoma regions are destroyed and its cells are dark in color. These
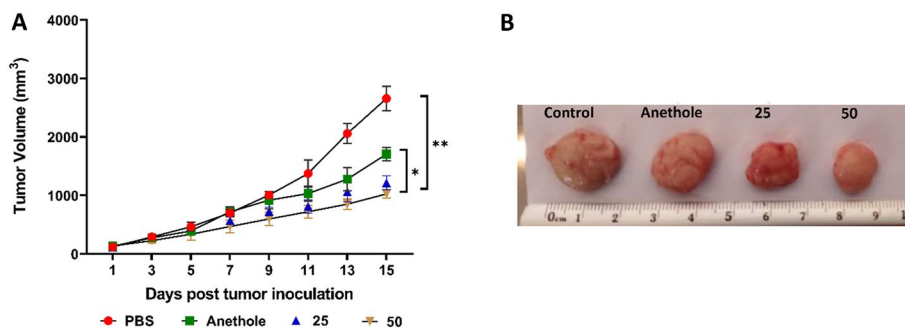

Fig. 4 Anti-tumor studies. **A** Results of tumor volume in mice treated with PBS, Ant, doses of 25 and 50 mg of Ant-BSA–CS–FA. **B** Macroscopic image of tumors removed on the day after injection of the formulations
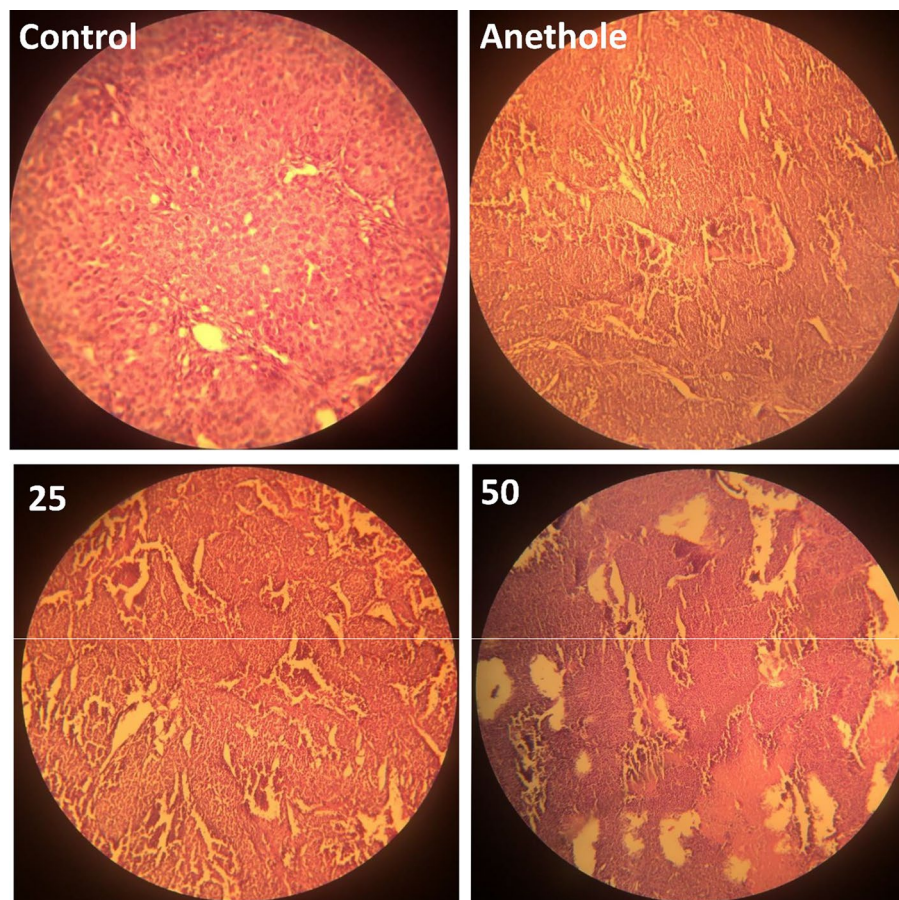
Fig. 5 Histological evaluations. H&E staining of the tumor sections from the control group, free Ant, doses 25 and 50 mg of the Ant-BSA–CS–FA

islets have undergone apoptosis and show apoptotic areas. As can be seen, in the sample treated with a concentration of 50 mg, the number of apoptotic islets is higher than in other groups. In the samples treated with nanoparticles, an increase in apoptotic areas is observed compared to the free drug, which shows the antitumor effects of the Ant in its nanoparticle form.

Discussion

In the present study, Ant was encapsulated in the BSA nanoparticles and these nanoparticles were surface coated with CS–FA. Some environmental factors, such as ultraviolet and visible light, temperature, atmospheric oxygen, and long-term storage significantly affect the chemical stability of Ant, which cause oxidation and isomeric reactions and finally destruction of it (Turek and Stintzing 2013). Hence, the formulation of such a drug could enhance its chemical stability. In addition, nanocarriers improve the drug solubility, and therapeutic index, as well as reduce the inhibitory effects on natural cells, and increase the effectiveness of the treatment (Kumari et al. 2016). In addition, by changing and modifying the surface of these carriers, controllable pharmacological and physicochemical properties can be achieved, as well as the ability to remove chemotherapy barriers (Ernest et al. 2018; Mashreghi et al. 2021b).

The high loading efficiency of BSA due to its ability to trap a large number of drug atoms in each molecule, biocompatibility and biodegradability, non-toxicity, non-immunogenicity, as well as specific absorption on tumor and inflamed tissue led to the selection of this carrier in the present study (Choukrani et al. 2021). Modification of nanoparticles, considering the type of nanoparticles, is an effective strategy to entrap drugs and suppress their side effects, and it can increase the drug concentration in the target organs or tissues, and then reduce the effective dose and adverse symptoms (Maiti et al. 2018). Therefore, in this study, to increase the efficiency of the nanocarrier, CS–FA was used to modify the surface of the nanoparticles. The binding of ligands, such as FA, transferrin, and Arg–Gly–Asp (RGD), etc. has been used in various studies to effectively identify and deliver drugs to cancer cells (Gu et al. 2017; Nik et al. 2021; Soe et al. 2019).

In this study, the desolvation method was used for the synthesis of nanoparticles, and CS attached to FA was conjugated to Ant-BSA–CS–FA. The average particle size was 252 nm, with a dispersion index of 0.28 and a zeta potential of 27.14 mV. The presence of a positive charge on the surface of nanoparticles can be attributed to the CS coating on the surface of nanoparticles. The presence of amine groups in the structure of CS increases the positive charge on the surface of nanoparticles, and this positive charge leads to an increase in the adhesion and retention of nanoparticles in cancer cells (Wang et al. 2013). On the other hand, the positive charge caused by the presence of CS on the surface of nanoparticles reduces the possibility of interaction of nanoparticles with phagocytes, which reduces the absorption of nanoparticles by these cells and increases their durability in the body (Parveen and Sahoo 2011). The use of FA in the structure of nanocarriers is one of the effective approaches in targeting and minimizing the accumulation of chemotherapy drugs in non-target organs (Li et al. 2014). FA is a non-toxic and non-immunogenic ligand that has a high tendency to bind to the surface of nanoparticles (Cheng et al. 2017). Considering that breast cancer cells have a high expression of FA receptors on their surface, therefore, in this study, to target drug delivery to cancer cells, FA binding to the surface of nanoparticles was done. FA has a negative charge, and it was shown that the attachment of FA to the surface of BSA nanoparticles can increase the surface negative charge (Sun et al. 2019). While in the present study, the surface zeta potential after modifying the surface of nanoparticles with CS–FA was reported to be positive, and this difference in charge can be attributed to the presence of CS coating. In addition, the results of a study showed that the use of FA on the surface of nanoparticles can enhance the active targeting effect of nanoparticles in cells with high expression of FA receptors, such as HeLa (Chu et al. 2021). In another study, the high-pressure homogeneous emulsification method was used for the synthesis of human serum albumin nanoparticles conjugated with glycyrrhizic acid containing resveratrol in which The EE% was 83.6% (Wu et al. 2017). Comparing the results of this study with the present study shows that the particle size and EE% are almost the same.

After characterizing and checking the percentage of drug encapsulation and ensuring success in the preparation of nanoparticles, the cytotoxicity of Ant-BSA–CS–FA against breast and colon cancer cells was evaluated compared to normal cells. The results show the safety of nanoparticles on normal cells at effective concentrations on cancer cells. The increased effect of nanoparticles on cancer cells can be attributed to the high expression of the FA receptor on the surface of the cells and the increased internalization of the

nanocarrier through receptor-mediated transfer. Since the amount of FA receptors on the surface of normal cells is much lower than that of cancer cells, it can be said that the modification of the surface of nanoparticles has an effective role in the targeted transfer and internalization of the drug to the investigated cancer cells. In a study, albumin–paclitaxel nanoparticles (FA–BSA–PTX) conjugated with FA were synthesized, and further investigation of the toxicity effect of nanoparticles on HeLa cells showed that FA can act as a targeting ligand for albumin carrier to enhance the active targeting effect of nanoparticles by expressing High FR is used (Chu et al. 2021). In another study, BSA nanoparticles conjugated with FA were used to increase the solubility, bioavailability, and transfer of baicalin to breast cancer cells, then the toxicity effects of nanoparticles were evaluated using MTT. The results of this study showed that compared to the control group and free baicalin, the synthesized nanoparticles inhibited the viability of MCF-7 cells. These results clearly showed that the encapsulation of baicalin in FA–albumin nanoparticles improves its antiproliferative activity (Liu et al. 2022).

Apoptosis activated by the mitochondrial-mediated intrinsic pathway is initiated by certain signaling molecules. When the permeability of the mitochondrial membrane changes, cytochrome c is released from the mitochondria into the cytosol. Upon receiving the apoptotic signal, caspase-9 is activated first, followed by caspase-3, -6, and -7, which ultimately leads to the cleavage of apoptosis-related protein substrates, and this is a process regulated by Bcl family proteins (Liu et al. 2022). Here, we found that the synthesized nanoparticles inhibited the expression of anti-apoptotic protein Bcl-2, increased the expression of pro-apoptotic protein BAX, and activated caspase-9, -3 in a dose-dependent manner, thereby causing It induces cell apoptosis.

In this study, the anticancer effects of Ant-BSA–CS–FA were investigated in a tumor-bearing mouse model. The results of this study showed a decrease in the volume of tumors during treatment with nanoparticles. In addition, the effect of nanoparticles on tumor tissue was investigated by H&E staining and the results showed the formation of apoptotic areas in the treated samples. In addition, it was found that the pro-apoptotic effects of nanoparticles on tumor tissue increase with increasing treatment concentration. Similar to the present study, in a study in 2019, the effects of albumin nanoparticles containing cabazitaxel conjugated with folate were investigated in tumor-bearing mice. The results of the study showed that nanoparticles containing FA show stronger fluorescence at the tumor site than nanoparticles without FA, which indicates an increase in delivery by FR-mediated endocytosis. In addition, the results showed that considering that the presence of nanoparticles is also confirmed in other tissues, such as the liver and kidney, the highest concentration is in tumor tissue. Examining the tumor volume in the free drug sample and two nanoparticle forms with FA and without FA showed that all three formulations inhibited tumor growth (Sun et al. 2019).

Conclusion

The results of this investigation showed the formation of Ant-loaded BSA nanoparticles surface-decorated with CS–FA. The side of Ant-BSA–CS–FA was 252 nm and had narrow dispersion, which indicates the formation of stable nanoparticles with an acceptable size for clinical applications. The surface charge of nanoparticles showed the presence of repulsive force to prevent the agglomeration of particles. Examining the toxicity effect

of Ant-BSA–CS–FA showed high toxicity of nanoparticles on breast and colon cancer cells compared to normal cells. Since the most toxicity was observed against breast cancer cells, more analyzes were performed to determine the inhibitory mechanism of nanoparticles. The results of the molecular analysis showed the activation of the internal pathway of apoptosis, which together with the anti-tumor effects of Ant-BSA–CS–FA that were shown in the tumor-bearing mouse model, showed the effectiveness of this formulation in inhibiting cancer cells. It introduces as a promising factor in preclinical and clinical investigations of cancer.

Declarations

Ethics approval and consent to participate
All institutional and national guidelines for the care and use of laboratory animals were followed.

Consent for publication
Not applicable.

Competing interests
The authors declare that they have no competing interests.

References

Agotegaray M, Campelo A, Zysler R, Gumilar F, Bras C, Minetti A, Massheimer V, Lassalle V (2016) Influence of chitosan coating on magnetic nanoparticles in endothelial cells and acute tissue biodistribution. J Biomater Sci Polym Ed 27(11):1069–1085

Aprotosoaie AC, Costache I-I, Miron A (2016) Anethole and its role in chronic diseases. In: Gupta S, Prasad S, Aggarwal B (eds) Drug discovery from mother nature, vol 929. Advances in experimental medicine and biology. Cham, Springer, pp 247–267

Auffan M, Rose J, Bottero J-Y, Lowry GV, Jolivet J-P, Wiesner MR (2009) Towards a definition of inorganic nanoparticles from an environmental, health and safety perspective. Nat Nanotechnol 4(10):634–641

Cé R, Marchi JG, Bergamo VZ, Fuentefria AM, Lavayen V, Guterres SS, Pohlmann AR (2016) Chitosan-coated dapsone-loaded lipid-core nanocapsules: growth inhibition of clinical isolates, multidrug-resistant *Staphylococcus aureus* and *Aspergillus* ssp. Colloids Surf A 511:153–161

Cheng L, Ma H, Shao M, Fan Q, Lv H, Peng J, Hao T, Li D, Zhao C, Zong X (2017) Synthesis of folate-chitosan nanoparticles loaded with ligustrazine to target folate receptor positive cancer cells. Mol Med Rep 16(2):1101–1108

Cho K, Wang X, Nie S, Chen Z, Shin DM (2008) Therapeutic nanoparticles for drug delivery in cancer. Clin Cancer Res 14(5):1310–1316

Choukrani G, Álvarez Freile J, Avtenyuk NU, Wan W, Zimmermann K, Bremer E, Dähne L (2021) High loading efficiency and controlled release of bioactive immunotherapeutic proteins using vaterite nanoparticles. Part Part Syst Charact 38(7):2100012

Chu Y, Chai S, Pan H, Qian J, Han C, Sui X, Liu T (2021) Preparation of folic acid-conjugated albumin nanoparticles containing paclitaxel using high-pressure homogenisation coagulation method. https://doi.org/10.21203/rs.3.rs-221888/v1

Dongare V, Kulkarni C, Kondawar M, Magdum C, Haldavnekar V, Arvindekar A (2012) Inhibition of aldose reductase and anti-cataract action of trans-anethole isolated from *Foeniculum vulgare* Mill. fruits. Food Chem 132(1):385–390

Ebrahimnejad P, Taleghani AS, Asare-Addo K, Nokhodchi A (2022) An updated review of folate-functionalized nanocarriers: a promising ligand in cancer. Drug Discov Today 27(2):471–489

Ernest U, Chen H-Y, Xu M-J, Taghipour YD, Asad MHHB, Rahimi R, Murtaza G (2018) Anti-cancerous potential of polyphenol-loaded polymeric nanotherapeutics. Molecules 23(11):2787

Fonte P, Nogueira T, Gehm C, Ferreira D, Sarmento B (2011) Chitosan-coated solid lipid nanoparticles enhance the oral absorption of insulin. Drug Deliv Transl Res 1:299–308

Frank L, Onzi G, Morawski A, Pohlmann A, Guterres S, Contri R (2020) Chitosan as a coating material for nanoparticles intended for biomedical applications. React Funct Polym 147:104459

Gonçalves MC, Mertins O, Pohlmann AR, Silveira NP, Guterres SS (2012) Chitosan coated liposomes as an innovative nanocarrier for drugs. J Biomed Nanotechnol 8(2):240–250

Greenwell M, Rahman P (2015) Medicinal plants: their use in anticancer treatment. Int J Pharm Sci Res 6(10):4103

Gu L, Shi T, Sun Y, You C, Wang S, Wen G, Chen L, Zhang X, Zhu J, Sun B (2017) Folate-modified, indocyanine green-loaded lipid-polymer hybrid nanoparticles for targeted delivery of cisplatin. J Biomater Sci Polym Ed 28(7):690–702

Hamedinasab H, Rezayan AH, Mellat M, Mashreghi M, Jaafari MR (2020) Development of chitosan-coated liposome for pulmonary delivery of *N*-acetylcysteine. Int J Biol Macromol 156:1455–1463

Huxley AJ, Griffiths M (1992) Dictionary of gardening. Stockton Press, New York

Jurado J, Alcazar A, Pablos F, Martín M (2006) LC determination of anethole in aniseed drinks. Chromatographia 64:223–226

Kratz F (2008) Albumin as a drug carrier: design of prodrugs, drug conjugates and nanoparticles. J Control Release 132(3):171–183

Kumari P, Ghosh B, Biswas S (2016) Nanocarriers for cancer-targeted drug delivery. J Drug Target 24(3):179–191

Lal M, Begum T, Gogoi R, Sarma N, Munda S, Pandey SK, Baruah J, Tamang R, Saikia S (2022) Anethole rich *Clausena heptaphylla* (Roxb.) Wight & Arn., essential oil pharmacology and genotoxic efficiencies. Sci Rep 12(1):9978

Li Y, Wu H, Yang X, Jia M, Li Y, Huang Y, Lin J, Wu S, Hou Z (2014) Mitomycin C-soybean phosphatidylcholine complex-loaded self-assembled PEG-lipid-PLA hybrid nanoparticles for targeted drug delivery and dual-controlled drug release. Mol Pharm 11(8):2915–2927

Liu F, Lan M, Ren B, Li L, Zou T, Kong Z, Fan D, Cai T, Cai Y (2022) Baicalin-loaded folic acid-modified albumin nanoparticles (FA-BSANPs/BA) induce autophagy in MCF-7 cells via ROS-mediated p38 MAPK and Akt/mTOR pathway. Cancer Nanotechnol 13(1):2

Maiti R, Panigrahi S, Yin T, Huo M (2018) Bovine serum albumin nanoparticles constructing procedures on anticancer activities. Int J Adv Res Biol Sci 5(4):226–239

Maleki MF, Jafari A, Mirhadi E, Askarizadeh A, Golichenari B, Hadizadeh F, Moghimi SMJ, Aryan R, Mashreghi M, Jaafari MR (2019) Endogenous stimuli-responsive linkers in nanoliposomal systems for cancer drug targeting. Int J Pharm 572:118716

Mashreghi M, Azarpara H, Bazaz MR, Jafari A, Masoudifar A, Mirzaei H, Jaafari MR (2018) Angiogenesis biomarkers and their targeting ligands as potential targets for tumor angiogenesis. J Cell Physiol 233(4):2949–2965

Mashreghi M, Faal Maleki M, Karimi M, Kalalinia F, Badiee A, Jaafari MR (2021a) Improving anti-tumour efficacy of PEGylated liposomal doxorubicin by dual targeting of tumour cells and tumour endothelial cells using anti-p32 CGKRK peptide. J Drug Target 29(6):617–630

Mashreghi M, Zamani P, Karimi M, Mehrabian A, Arabsalmani M, Zarqi J, Moosavian SA, Jaafari MR (2021b) Anti-epithelial cell adhesion molecule RNA aptamer-conjugated liposomal doxorubicin as an efficient targeted therapy in mice bearing colon carcinoma tumor model. Biotechnol Prog 37(3):e3116

Mirhadi E, Mashreghi M, Maleki MF, Alavizadeh SH, Arabi L, Badiee A, Jaafari MR (2020) Redox-sensitive nanoscale drug delivery systems for cancer treatment. Int J Pharm 589:119882

Mohanta V, Madras G, Patil S (2012) Layer-by-layer assembled thin film of albumin nanoparticles for delivery of doxorubicin. J Phys Chem C 116(9):5333–5341

Nik ME, Jaafari MR, Mashreghi M, Nikoofal-Sahlabadi S, Amin M, Sadeghnia HR, Iranshahi M, Navashenaq JG, Malaekeh-Nikouei B (2021) The effect of RGD-targeted and non-targeted liposomal Galbanic acid on the therapeutic efficacy of pegylated liposomal doxorubicin: from liposomal preparation to in-vivo studies. Int J Pharm 604:120710

Parveen S, Sahoo SK (2011) Long circulating chitosan/PEG blended PLGA nanoparticle for tumor drug delivery. Eur J Pharmacol 670(2–3):372–383

Ponte EL, Sousa PL, Rocha MV, Soares PM, Coelho-de-Souza AN, Leal-Cardoso JH, Assreuy A (2012) Comparative study of the anti-edematogenic effects of anethole and estragole. Pharmacol Rep 64(4):984–990

Rhee Y-H, Chung P-S, Kim S-H, Ahn JC (2014) CXCR4 and PTEN are involved in the anti-metastatic regulation of anethole in DU145 prostate cancer cells. Biochem Biophys Res Commun 447(4):557–562

Satapathy S, Patro CS, Patro G, Panda M, Patra A (2023) Cancer therapy. J Pharm Negat Results 14:3643–3649

Soe ZC, Kwon JB, Thapa RK, Ou W, Nguyen HT, Gautam M, Oh KT, Choi H-G, Ku SK, Yong CS (2019) Transferrin-conjugated polymeric nanoparticle for receptor-mediated delivery of doxorubicin in doxorubicin-resistant breast cancer cells. Pharmaceutics 11(2):63

Subia B, Kundu S (2012) Drug loading and release on tumor cells using silk fibroin–albumin nanoparticles as carriers. Nanotechnology 24(3):035103

Sun Y, Zhao Y, Teng S, Hao F, Zhang H, Meng F, Zhao X, Zheng X, Bi Y, Yao Y (2019) Folic acid receptor-targeted human serum albumin nanoparticle formulation of cabazitaxel for tumor therapy. Int J Nanomed 14:135

Tian J, Liu J, Tian X, Hu Z, Chen X (2004) Study of the interaction of kaempferol with bovine serum albumin. J Mol Struct 691(1–3):197–202

Turek C, Stintzing FC (2013) Stability of essential oils: a review. Compr Rev Food Sci Food Saf 12(1):40–53

Wang Y, Li P, Kong L (2013) Chitosan-modified PLGA nanoparticles with versatile surface for improved drug delivery. AAPS PharmSciTech 14:585–592

Watkins R, Wu L, Zhang C, Davis RM, Xu B (2015) Natural product-based nanomedicine: recent advances and issues. Int J Nanomed 10:6055

Wei Y, Li L, Xi Y, Qian S, Gao Y, Zhang J (2014) Sustained release and enhanced bioavailability of injectable scutellarin-loaded bovine serum albumin nanoparticles. Int J Pharm 476(1–2):142–148

Wu M, Lian B, Deng Y, Feng Z, Zhong C, Wu W, Huang Y, Wang L, Zu C, Zhao X (2017) Resveratrol-loaded glycyrrhizic acid-conjugated human serum albumin nanoparticles wrapping resveratrol nanoparticles: Preparation, characterization, and targeting effect on liver tumors. J Biomater Appl 32(2):191–205

Xu R, Fisher M, Juliano R (2011) Targeted albumin-based nanoparticles for delivery of amphipathic drugs. Bioconjug Chem 22(5):870–878

Zimmermann-Klemd AM, Reinhardt JK, Winker M, Gründemann C (2022) Phytotherapy in integrative oncology—an update of promising treatment options. Molecules 27(10):3209

Publisher's Note